J. Fluid Mech. (1990), *vol.* 218, *pp.* 601–617
Printed in Great Britain

The breakup of viscous jets with large velocity modulations

By D. W. BOUSFIELD†, I. H. STOCKEL AND C. K. NANIVADEKAR‡
Department of Chemical Engineering, University of Maine, Orono, ME 04469, USA

(Received 12 September 1989)

The surface-tension-driven breakup of viscous jets is observed for a range of Weber and Ohnesorge numbers. The breakup is enhanced with a sinusoidal modulation or pulsation of the jet's exit velocity; the velocity modulation amplitudes and wavenumbers are larger than previous values reported in the literature. The combinations of modulation amplitude and wavenumber that produce uniform droplets are identified for each pair of Weber and Ohnesorge numbers. Satellite droplets are eliminated at values of the Ohnesorge number greater than 1.6. Droplet pairing and merging occurs at high wavenumbers; droplet merging has not been reported in the jet breakup literature. The timescale for breakup is predicted within the data scatter by the thin filament equation of Bousfield *et al.* (1986) with no fitted parameters. An upper bound on satellite droplet size is predicted by the thin-filament equation and the average satellite droplet volume is qualitatively predicted. An algebraic expression is derived to predict the breakup time of viscous jets with large velocity modulation amplitudes.

1. Introduction

The surface-tension-driven breakup of liquid filaments into droplets is an important step in a variety of processes; some of these processes have been enumerated by Schummer & Tebel (1982). The motivation for this work is related to the spraying of viscous kraft black liquors into recovery boilers. Most of the recent work in this area has been stimulated by the need of uniform droplets in ink jet printers. The breakup of Newtonian filaments has been reviewed by Bogy (1979*b*) and McCarthy & Molloy (1974). The initial disturbances to the jet at the nozzle used by previous investigators are generally small and not well characterized; most of this past work has been with low-viscosity liquids such as water and the filament breakup lengths were calculated once the initial disturbance amplitude was fitted to the data. A fundamental understanding of the surface-tension-driven breakup of viscous jets is only possible if the initial disturbance to the jet is well quantified. A sinusoidal pulsation or modulation of the jet's exit velocity provides a well-characterized initial disturbance to the jet.

A number of experiments have been conducted to study the effect of the different parameters such as viscosity, surface tension, jet velocity, and nozzle diameter. The viscosities of past work cover the range of 0.01 P (water) to 6.0 P. Controlled jet breakup has been reported using low-amplitude oscillation of the nozzle, or in the

† To whom correspondence should be addressed.
‡ Present address: Hercules Research Center, Wilmington, DE 19894, USA.

flow rate, or on the jet surface. Plateau (1873) was the first to show that a disturbance of wavelength greater than the circumference of the jet grows with time. Schneider & Hendricks (1964) vibrated the nozzle using a pulsating piezoelectric transducer; uniform water droplets were obtained for a given range of frequencies. Rutland & Jameson (1970), Goedde & Yuen (1970), Rajagopalan & Tien (1973), and Kurabyashi & Karasawa (1982) used transverse nozzle vibrations to enhance the jet breakup; the initial conditions for these studies are not described in detail in the papers. Araki & Masuda (1978) used longitudinal nozzle vibrations to control the breakup of water jets. Pimbley & Lee (1977), Sakai *et al.* (1982), Schummer & Tebel (1982) and Taub (1975) used small longitudinal nozzle vibrations to control droplet formation; the amplitudes of the vibrations and the initial conditions are generally not well defined in these studies. Non-sinusoidal velocity modulations were shown to eliminate satellite droplets for water by Chaudhary & Maxworthy (1980*a*, *b*); the initial conditions were known once the data was fitted to the model but concern was expressed in the paper about the nozzle creating extraneous harmonic additions to the imposed disturbance.

Rayleigh (1879) first analysed the breakup of inviscid filaments using linear stability theory. He assumed an equivalence between spatial and temporal growth of disturbances, and thus calculated the growth of infinitesimal periodic disturbances on a stationary liquid cylinder. This approach precludes any consideration of velocity profile rearrangement on the jet in the neighbourhood of the nozzle and it assumes that the disturbance wavelength remains constant as the disturbances evolves. Weber (1931), Sterling & Sleicher (1975) and others have followed Rayleigh's basic approach, limited to the early stages of the disturbance growth; satellite formation is not predicted by the linear theories.

Yuen (1968), Wang (1968), Nayfeh (1970), Lee (1974) and Lafrance (1975) present nonlinear analyses for the breakup of jets; viscosity was neglected but the occurrence of satellite droplets was first seen. A nonlinear model of the fluid mechanics in two dimensions was used by Shokoohi (1976). However, the initial conditions of his work were limited to surface disturbances. Chaudhary & Redekopp (1980) give a third-order solution with initial conditions in the form of an axial velocity profile; their solution neglects viscosity. Viscosity is not included in the third-order theory presented by Busker, Lamers & Nieuwenhuizen (1989).

One-dimensional theories have been successful in the description of filament breakup with known surface or velocity initial conditions. The Cosserat equation was developed by Green (1976) and was used by Bogy (1978) to describe the breakup of viscous jets. The Cosserat equation is developed *ab initio* as a one-dimensional theory and contains other one-dimensional approximations obtained from the full Navier–Stokes equations. The velocity profile rearrangement at the nozzle is neglected. Bogy (1979*a*) used a third-order perturbation analysis to describe the breakup of an inviscid jet. Bogy, Shine & Talke (1980) solved the full spatial problem numerically and was able to describe the satellite formation with viscous jets. The computational time for the spatial problem was large, especially for viscous jets with long breakup lengths.

The thin-filament equation of Bousfield *et al.* (1986) predicts the satellite droplet size reported by Lafrance (1975) and Rutland & Jameson (1970), the jet shape reported by Goedde & Yen (1970), and the growth of the high harmonics by Taub (1975). The thin-filament equation is obtained by a formal averaging of quantities across the filament radius or is obtained from the Cosserat equation through a spatial integration when the filament radius is smaller than the disturbance lengthscale.

Bousfield *et al.* (1986) showed that the thin-filament equations agree with the two-dimensional solution of the full axisymmetric Navier–Stokes equations; the two-dimensional solution was computed with a transient finite-element algorithm described by Keunings (1986). The thin-filament equation has been extended to describe non-Newtonian filament breakup and the breakup of stretching filaments between plates (see Bousfield 1988). It provides an efficient nonlinear solution to the surface-tension-driven breakup problem which includes viscous effects and accepts arbitrary initial velocity or surface profiles.

An estimate of the filament breakup time was given by Bousfield & Denn (1987) for small velocity modulations. An equation was derived to estimate the initial surface disturbance from a given velocity modulation amplitude. With this initial surface disturbance, linear stability analysis can be used to estimate the breakup time. The generation of capillary instabilities on a liquid jet was described by Leib & Goldstein (1986), who examined the coupling between disturbances and capillary instabilities in a liquid jet. A 'coupling coefficient' was used to quantify this relationship.

In this paper, the surface-tension-driven breakup of viscous filaments is reported for a range of Weber and Ohnesorge numbers. A stacked piezoelectric transducer drives a piston in a minimum-volume chamber upstream of a nozzle with a small length-to-diameter ratio. The experimental work is unique in that the initial velocity of the jet is well characterized and the amplitude of modulation is larger than previously described. Regions of velocity amplitude and wavenumber that produce uniform droplets are described. Satellite droplets are eliminated for values of the Ohnesorge number greater than 1.6. Droplet merging and pairing are observed at large wavenumbers. The filament breakup time is predicted, within the scatter of the data, by the thin-filament equation. The correct order of magnitude of the satellite volume is calculated by the thin-filament equation. An algebraic expression is given to estimate the timescale for breakup of viscous jets with large velocity modulations.

2. Experiments

A 0.04 m^3 capacity syringe was used to provide a non-pulsating flow with a known volumetric flow rate to the nozzle assembly. The nozzle assembly was constructed from stainless steel and is schematically represented in figure 1. A stacked piezoelectric transducer moved a piston in a minimum-volume chamber. The piezoelectric transducer mechanically expanded or contracted in response to the input voltage; the degree of movement for a given voltage was known from calibration. With the movement of the piston, the jet exit velocity was changed in time around an average jet velocity; the exit velocity at any point of time was equal to the average jet velocity in addition to the velocity caused by the movement of the piston. An adjustable radial gap created a large pressure drop into the chamber to dynamically isolate the syringe from the nozzle. The nozzle diameter was 1.54 mm and had the length-to-diameter ratio of 0.1. Mass was added to the nozzle face to add mechanical stiffness to the assembly and to lower the resonant frequency of the nozzle assembly.

The experiments were computer controlled to change the velocity modulation amplitude and the wavenumber. A waveform generator sent a sinusoidal voltage to the piezoelectric transducer through an amplifier. The actual voltage sent to the piezoelectric transducer was known. A video camera–strobe system recorded the resulting filament breakup at a given camera position relative to the nozzle exit; a

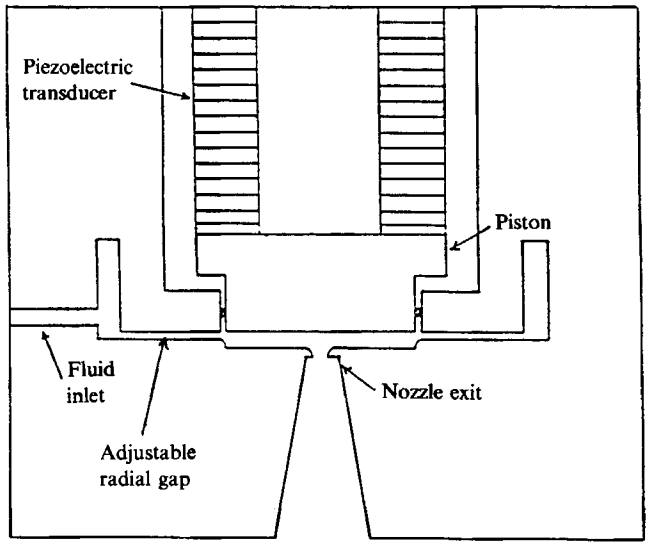

FIGURE 1. Schematic of the nozzle assembly.

microscope was inserted into the video camera optics to enlarge the image. A calibrated grid inside the microscope measured the droplet dimensions.

Four dimensionless groups were systematically investigated by the experimental program: the wavenumber k, Ohnesorge number Oh, and Weber number We, and the velocity modulation amplitude F. These groups are defined as follows:

$$k = \pi df/V, \tag{1a}$$

$$Oh = \mu/(\rho\sigma d)^{\frac{1}{2}}, \tag{1b}$$

$$We = V^2\rho d/\sigma, \tag{1c}$$

$$F = (V_{\max} - V)(\rho d/\sigma)^{\frac{1}{2}}, \tag{1d}$$

where d is the jet diameter, f is the frequency of modulation, V is the average jet velocity, and $V_{\max}$ is the maximum jet velocity at the nozzle exit during a flow pulsation. The viscosity, density, and surface tension of the liquid are μ, ρ, and σ, respectively. Five values of the Ohnesorge number and three values of the Weber number were studied. For each combination of these two groups, the wavenumber was changed between 0.26 and 1.34. At each wavenumber, a number of velocity modulations were tested. A number of camera positions from the nozzle to the longest breakup length had to be obtained to produce a picture of the entire breakup process.

The jet's initial diameter was taken to be the same as the nozzle diameter for the calculations of the wavenumber, Ohnesorge number and Weber number. The jet diameter at the nozzle was observed to be 1.6 mm. The swelling of the jet should have little impact on the calculation of the dimensionless groups.

The time for filament breakup is made dimensionless as follows:

$$T_{\text{break}} = t(\sigma/\rho d^3)^{\frac{1}{2}}, \tag{2}$$

where t is the actual time for breakup (the breakup length divided by the jet

velocity). The distortion of the filament surface at any location along the jet is characterized by the dimensionless surface disturbance amplitude given by

$$\epsilon = (R_{\min} - R)/R, \tag{3}$$

where $R_{\min}$ and R are the minimum filament radius at any location and the initial filament radius, respectively. The volume of liquid contained in satellite droplets is expressed in terms of the percent volume of the total liquid volume.

Known weight percent glycerin–water mixtures were used as the test liquid. The viscosity was measured with a glass bulk capillary rheometer. The surface tension and the density were determined from established data on glycerin–water mixtures (Weast 1975).

The amplitude of the velocity modulation was calculated from the input voltage. The mechanical response of the piezoelectric transducer to an applied voltage is known and therefore the movement of the piston was determined. This movement was used to calculate the velocity amplitude for a given frequency of modulation and liquid flow rate.

3. Experimental results

Figures 2–6 summarize the experimental results of this work for a jet velocity of 13 m/s or a Weber number of 5000. The limits of the collected data are shown by a dotted border in each figure. The shaded regions are the conditions which produced uniform droplets. The open circles represent the conditions where the jet remained unbroken until it contacted the liquid collection area. The filled squares are the upper limits where the droplets will not merge. The data for the other two Weber numbers can be found in Stockel (1988): similar results are obtained.

Uniform droplet formation (droplets of the same size with no stray or satellite droplets present) is limited at $Oh = 0.40$ and $Oh = 0.85$ because of the formation of satellite droplets at the low wavenumbers. Satellite droplets are not formed when the Ohnesorge number is greater than 1.6 at the lowest wavenumber studied ($k = 0.26$). Satellite droplet volume decreases as the Ohnesorge number increases from 0.40 to 0.85. Figures 7 (*a*) and 7 (*b*) show examples of the resulting droplet formation for a low and a high Ohnesorge number. At low Ohnesorge numbers, satellite droplets are formed by the nonlinear mechanism previously described in the literature. At high values, a drop–thread configuration is produced as in figure 7*b*, which is similar to that observed with viscoelastic jets (see Goldin *et al.* 1969). This drop-thread configuration breaks with the thread being drawn into one of the main droplets.

Uniform droplet formation of a target size is limited at high wavenumbers and amplitudes by pairing and merging of droplets. An example of merging is illustrated in figure 7 (*c*); the trailing drop catches the lead drop and they merge. Uniform droplets are formed but they are twice the expected size.

Stray droplets are formed at high values of the Ohnesorge number and velocity modulation. This may be an artifact of the experimental technique. The conditions for stray droplet production do not follow a regular pattern.

Droplets are formed at wavenumbers much greater than one. Figures 2 and 3 show several conditions where droplets are produced with wavenumbers in the range of 1.0 to 1.23. Uniform, non-merging droplets are produced in figure 2 at a wavenumber of 1.15. Chaotic drop formation or merging droplets, however, is characteristic of the high-wavenumber conditions. Experiments were conducted up to a wavenumber of 1.56 and droplets were formed, but the droplets either merged or the results were

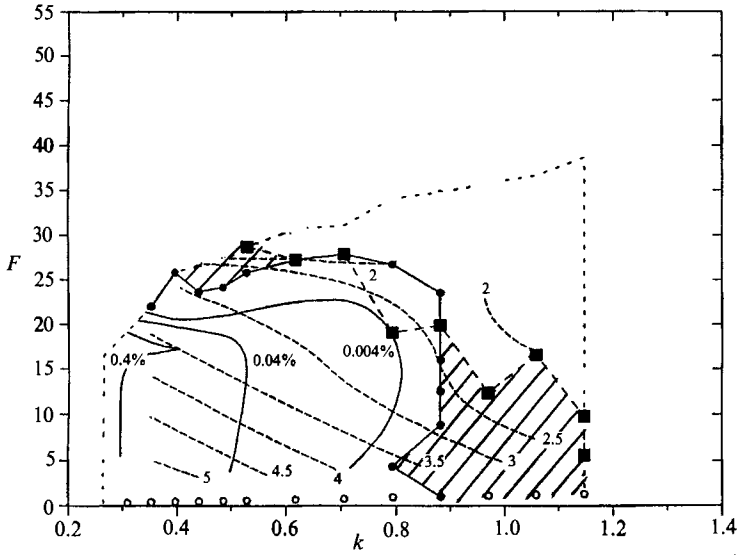

FIGURE 2. Experimental results for $Oh = 0.4$ and $We = 5000$. The solid lines are the volume percent of the liquid contained in satellite droplets. The broken lines are the dimensionless breakup times. The dotted line is the region of collected data. Shaded areas are the regions of uniform droplet formation. ■—■, Drops will not merge; ●—●, no satellites; ○, jet not broken.

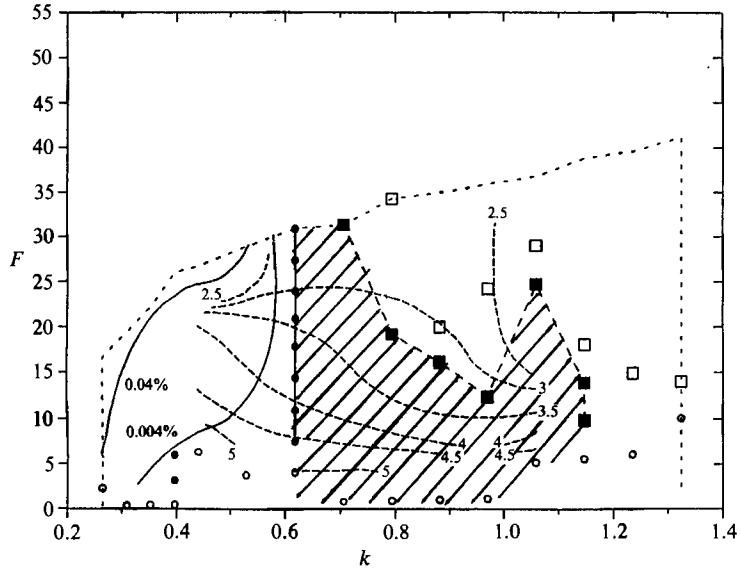

FIGURE 3. As figure 2 but at $Oh = 0.8$. ■—■, Drops will not merge; □, drops will merge and/or chaotic; ●—●, no satellites; ○, jet not broken.

chaotic. Droplets formed at wavenumbers of this magnitude have not been reported in the literature because the modulation amplitude has not been large enough previous to this study.

The solid lines in figures 2 and 3 are contours of the satellite volumes obtained at the camera position farthest from the nozzle. No satellites were formed in figures 4–6. Satellite droplets are not consistently formed: some video frames have more than one

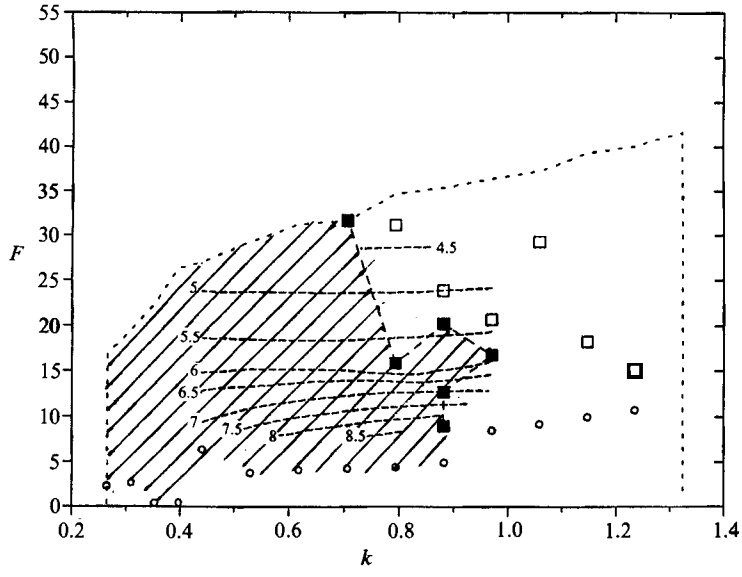

FIGURE 4. As figure 2 but at $Oh = 1.6$. ■—■, Drops will not merge; □, drops will merge and/or chaotic; ○, jet not broken.

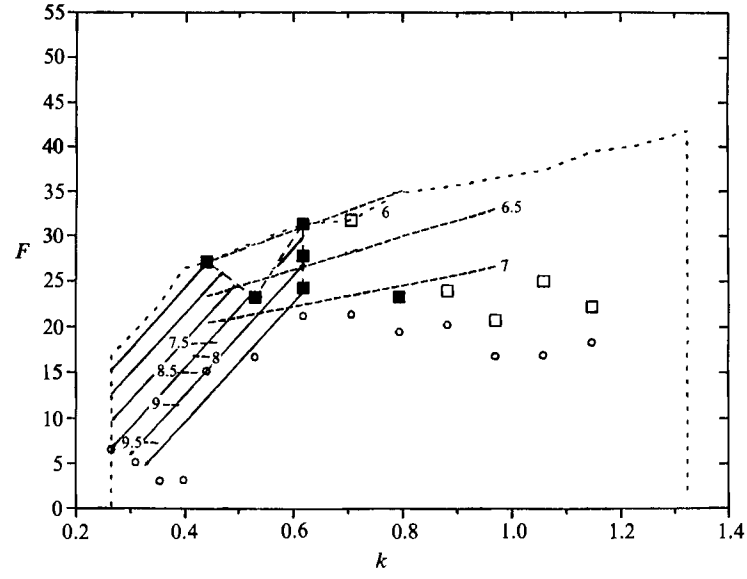

FIGURE 5. As figure 2 but at $Oh = 2.2$. ■—■, Drops will not merge; □, drops will merge and/or chaotic; ○, jet not broken.

satellite droplet and others have none. This randomness is due to the aerodynamic interactions of the small droplets and the merging of the satellite droplets with the main drops. The reported satellite volume is an average value from 20 video frames.

The broken lines in figure 2–6 give the dimensionless breakup time. The breakup time is determined by the average camera position where breakup occurred divided by the jet velocity. The breakup time generally decreases with increasing velocity modulation amplitude. As expected, large Ohnesorge numbers give large breakup times.

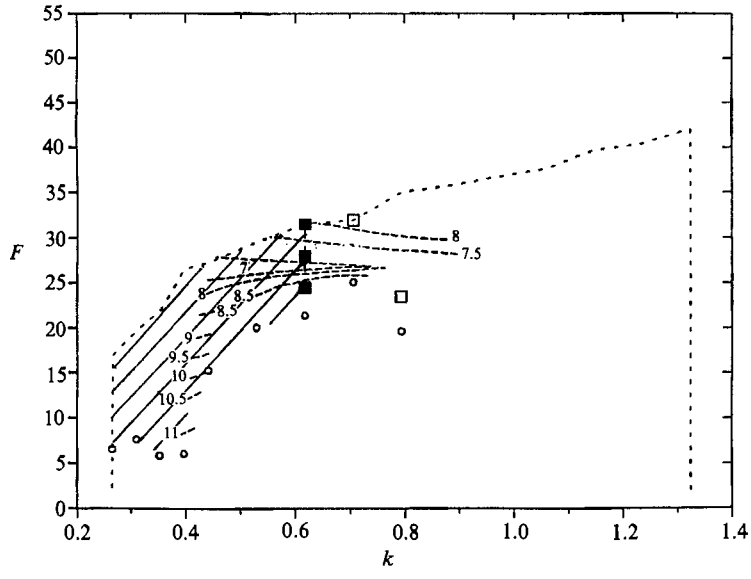

FIGURE 6. As figure 2 but at $Oh = 2.8$. ■—■, Drops will not merge; □, drops will merge and/or chaotic; ○, jet not broken.

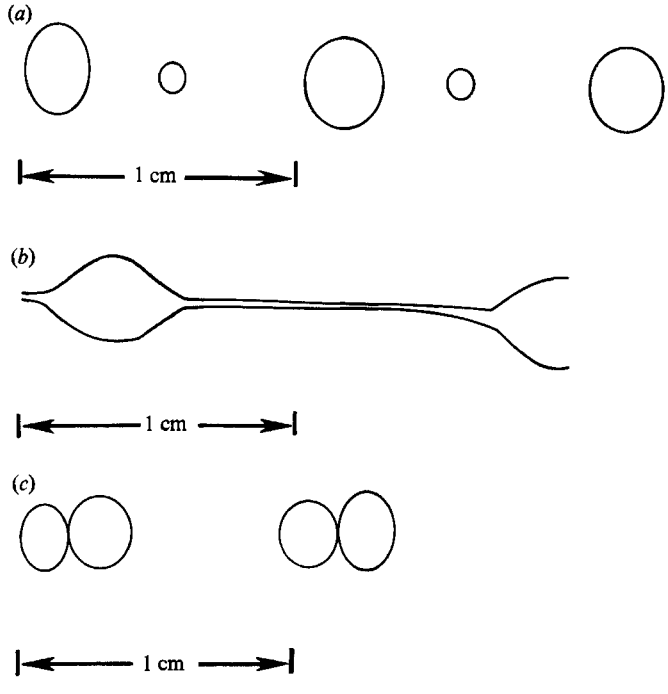

FIGURE 7. Traces from videographs to show examples of (*a*) satellite droplet formation for $Oh = 0.4$, $k = 0.497$, $We = 1260$, and $F = 33$; (*b*) no satellite droplet formation for $Oh = 2.8$, $k = 0.29$, $We = 1330$, and $F = 12$; (*c*) droplet merging for $Oh = 1.6$, $k = 1.1$, $We = 1330$, and $F = 33$.

4. Discussion of the results

Goedde & Yuen (1970) observed that the volume of liquid between main droplets decreases as the liquid viscosity increases. This observation is sysmematically demonstrated by the data. The drop–thread configuration is formed, which slows down the breakup process. The liquid in these filaments has time to drain into the neighbouring droplets. The filaments typically break near the midpoint between the main droplets as in figure 7(*b*). The filaments contract into the main droplet as described by Goedde & Yuen (1970).

The merging of droplets limits the production of uniform droplets at high wavenumbers, especially at high values of the Ohnesorge number. Droplet merging is likely to be caused by different drag forces on 'leading' and 'trailing' droplets. The lead drop creates an aerodynamic disturbance for the trailing drop. The trailing drop therefore has less aerodynamic drag and does not decelerate as rapidly as the lead drop. Small disturbances will start this merging pattern. See Stockel (1988) for a detailed discussion of the aerodynamics around droplet trains.

Another explanation for merging, especially at high Ohnesorge numbers or high wavenumbers, may be the pull on a drop exerted because of surface tension by a filament still connected to the drop. If the breakup of the filament between droplets is not exactly symmetrical, surface-tension forces will impart a velocity to the droplet. At high wavenumbers, the growth rate of the disturbance is small and a slight non-symmetric breakup could allow surface-tension forces to pull droplets relative to the average droplet velocity. These surface-tension forces could explain the droplet pairing seen in figure 7(*c*). This mechanism can be pictured from figure 7(*b*) and the consolidation of the filament with the droplet has been discussed by Goedde & Yuen (1969).

The source of stray off-axis droplets is not clear. They may be the remains of the filament between droplets which get thrown off-axis by the aerodynamic forces. Vortex shedding behind cylinders has been studied for many years and is known to produce transverse velocity fluctuations (see Pao & Kao 1977). The small filament fragments could be displaced off-axis by these transverse velocity components. Achenbach (1974) described the complex vortex configuration in the wake of a sphere at high Reynolds numbers. This vortex configuration may be responsible for moving the filament material between drops to a random off-axis position. The possible effects of lift and drag on droplets are discussed by Stockel (1988).

5. Comparison with the thin-filament equation

The dimensionless breakup times and the satellite droplet volumes are compared with the results of the thin-filament equation given in Bousfield *et al.* (1986). The initial radius and velocity profile in one wavelength of the disturbance are

$$r = 1, \tag{4a}$$

$$u = (F\,Oh\,k/\pi)\sin(2\pi z/\lambda), \tag{4b}$$

where z is the axial coordinate and λ is the wavelength of the disturbance. The radius is made dimensionless with the initial jet radius and the velocity is made dimensionless with the group $\mu d/\sigma\lambda$. These initial conditions correspond to an undeformed cylinder with a prescribed sinusoidal velocity profile. The actual initial conditions imposed on the jet by the motion of the piston is not known, but the

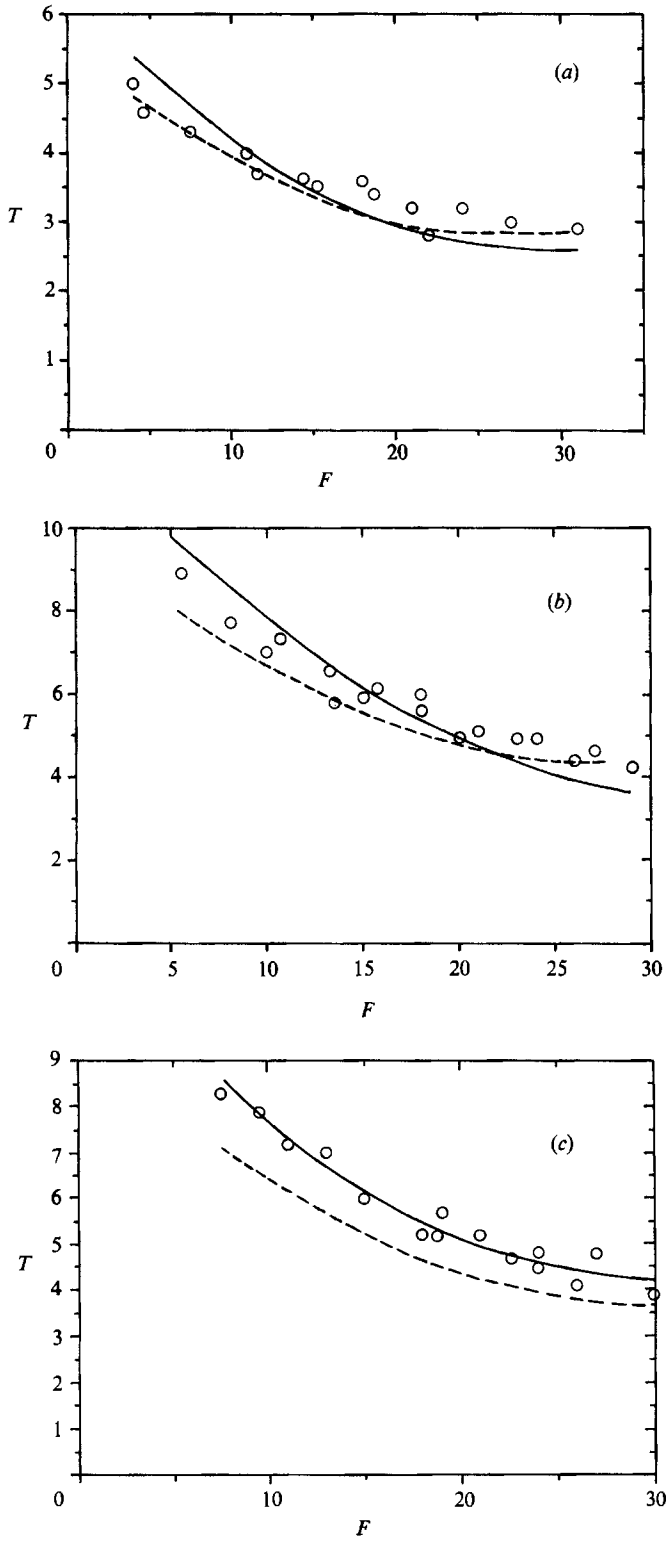

FIGURE 8 (*a–c*). For caption see facing page.

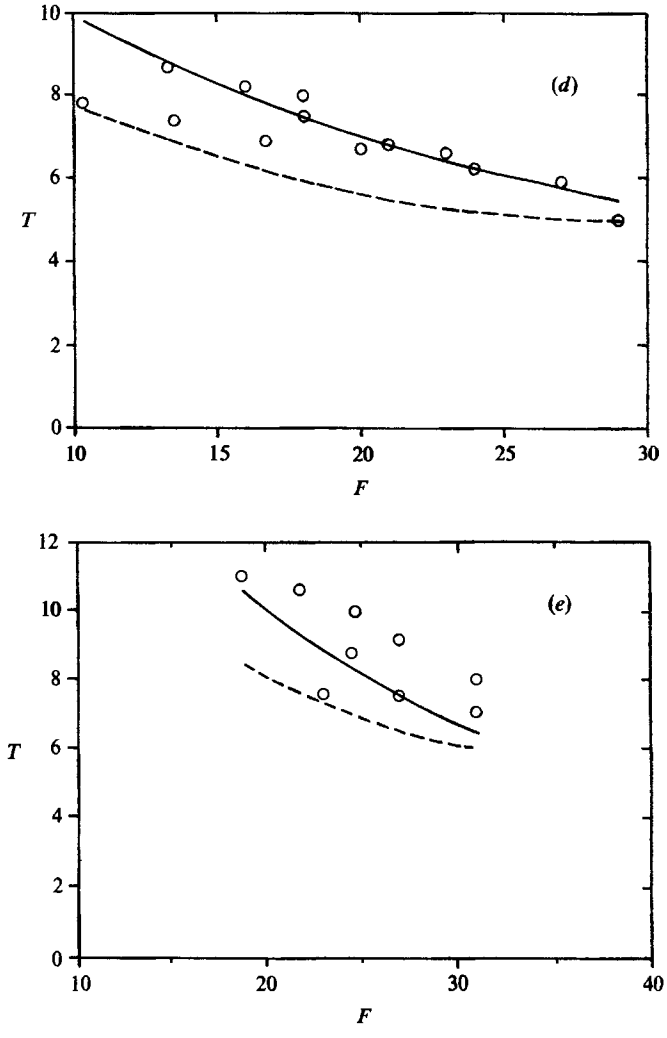

FIGURE 8. Comparison of the dimensionless breakup time between experimental results (open symbols), the thin filament (solid line), and the algebraic expression (broken line) for (*a*) $k = 0.62$, $Oh = 0.89$; (*b*) $k = 0.44$, $Oh = 1.72$; (*c*) $k = 0.62$, $Oh = 1.72$; (*d*) $k = 0.44$, $Oh = 2.26$; (*e*) $k = 0.62$, $Oh = 2.96$.

comparison between the thin-filament predictions and the experiments indicates that (4*b*) is accurate. The dimensionless groups in the thin-filament equation are formed from the Ohnesorge number and the wavenumber as

$$\alpha = k/\pi, \tag{5a}$$

$$\beta = \tfrac{1}{2}(\pi/k\,Oh)^2. \tag{5b}$$

The solid lines in figure 8(*a–e*) are the breakup time predictions by the thin-filament equation. The open circles are the data collected at all three Weber numbers and the given Ohnesorge number. The broken line is the result of an approximate analysis given later in this paper. The velocity modulation amplitude, the wavenumber, and the Weber and Ohnesorge numbers are all determined independently in the experiment. There is no fitted parameter in the thin-filament

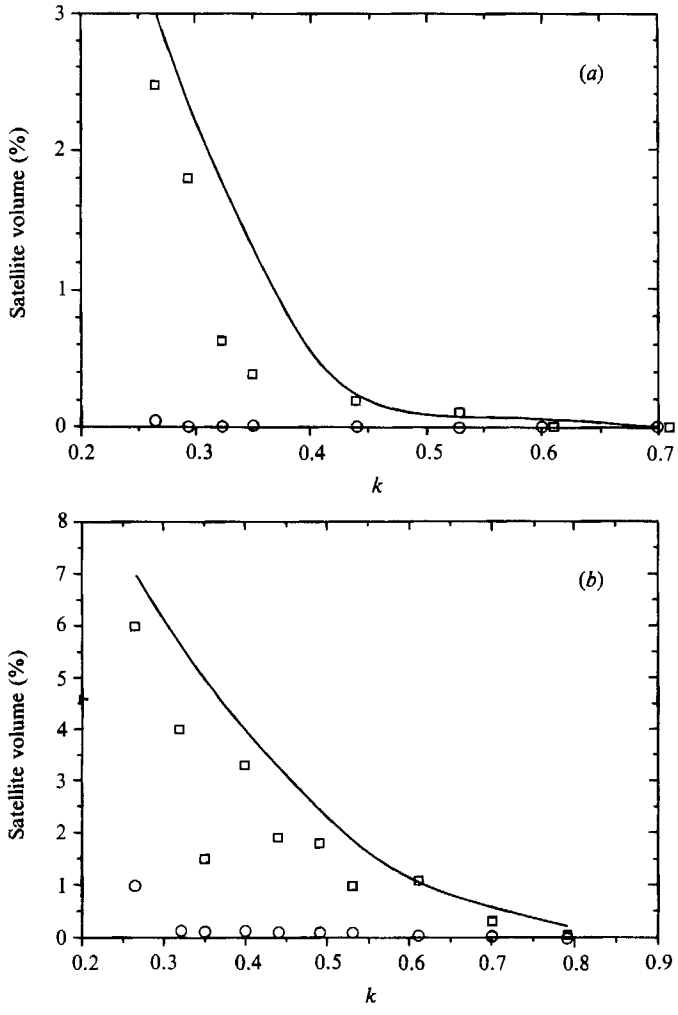

FIGURE 9. Satellite volume percent obtained for $F = 5.0$, and $We = 5000$. The circles are the averaged satellite volume, the squares are the maximum satellite volume, and the solid line is the result of the thin filament equation. (*a*) $Oh = 0.4$; (*b*) $Oh = 0.88$.

equation to match the data; the initial conditions are well characterized. The aerodynamics do not strongly affect the breakup times at these Weber numbers: the disturbance growth factor does not change when these Weber numbers are inserted into Weber's equation with the correction of Sterling & Sleicher (1975). The thin-filament equation predicts the breakup time within the scatter of the data.

The resulting satellite volume is qualitatively predicted by the thin-filament equation. Figures 9(*a*) and 9(*b*) compare the satellite volume fraction predicted by the thin filament equation and that obtained experimentally for the two lowest Ohnesorge numbers with a velocity modulation amplitude near five; the circles represent the average satellite volume and the squares represent the maximum satellite observed. The thin-filament equation predicts the maximum satellite droplet size observed. The over prediction of the average droplet size by the thin-filament equation is caused by the merging of potential satellite droplets with the main droplets.

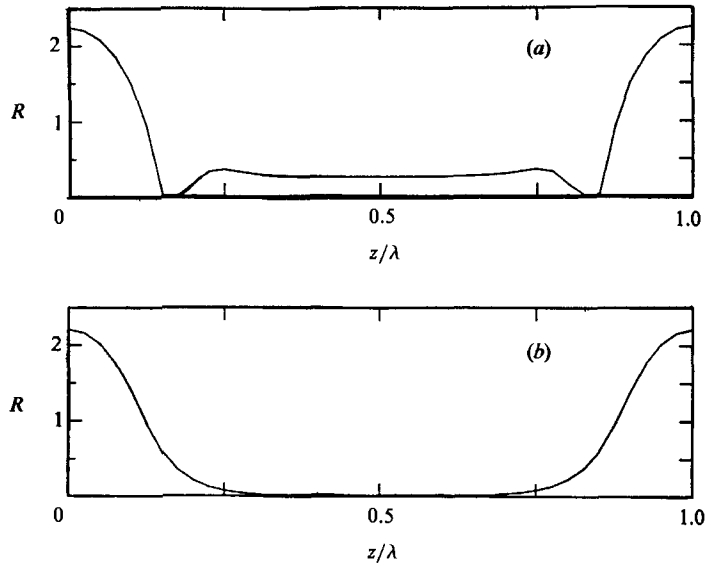

FIGURE 10. The shape of the jet near breakup predicted by the thin-filament equation for (*a*) the conditions of figure 7(*a*); (*b*) the conditions of figure 7(*b*).

The thin-filament equation predicts the elimination of satellite droplets near an Ohnesorge number of 1.2 at a wavenumber of 0.26. The elimination of satellite droplets at high Ohnesorge numbers is explained by the thin-filament equation. Figures 10(*a*) and 10(*b*) are the filament shape predicted by the thin-filament equation for the conditions represented in figures 7 (*a*) and 7 (*b*). At the low Ohnesorge number, liquid is left between the droplets because of the inertia of the liquid. At the high Ohnesorge number, the filament thins and forms the drop–thread configuration; the thin-filament equation predicts that the thread breaks at the midpoint between the main drops. This thread is drawn into the main droplets by surface tension forces.

5. Estimation of breakup time

Bousfield & Denn (1987) present an expression to estimate breakup time for small values of the velocity modulation amplitude. Their expression uses linear stability theory in combination with an equation to preduct the initial surface disturbance amplitude from the velocity modulation amplitude. Their equation, in terms of the above dimensionless parameters, becomes

$$T_{\text{break}} = -\ln(\epsilon_0)/\theta, \tag{6a}$$

$$\epsilon_0 = 1 - \exp(-F/12\,Oh\,k), \tag{6b}$$

$$\gamma = [36k^4 Oh^2 - 4k^2(1-k^2)]^{\frac{1}{2}} - 6k^2 Oh, \tag{6c}$$

where ϵ_0 estimates the initial surface disturbance created by a modulation of the jet exit velocity and γ is the dimensionless disturbance growth factor obtained from linear stability theory using the approximation for the Bessel function for small wavenumbers (see Sterling & Sleicher). Figure 11 illustrates how the surface disturbance amplitude predicted by this expression compares with the thin-filament equation for small velocity modulation amplitudes: the breakup time is predicted within 10% of the value obtained from the thin-filament equation.

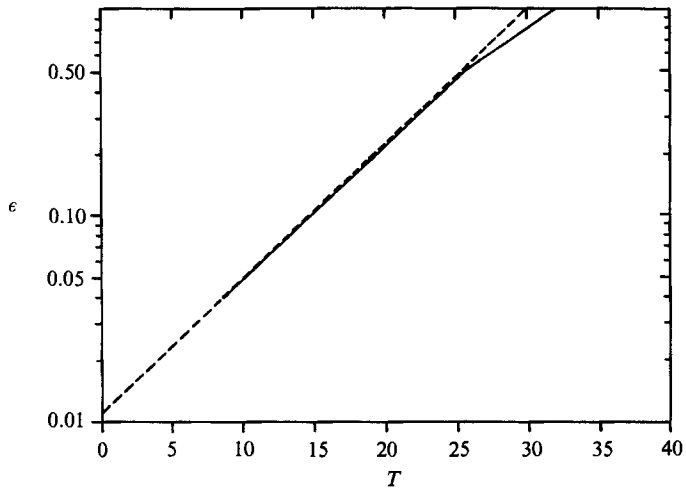

FIGURE 11. The growth of the surface disturbance amplitude with time. The solid line is the result using the thin-filament equation and the broken line is the result using the expression of Bousfield & Denn.

The expression by Bousfield & Denn (1987) does not work well for large values of the velocity modulation amplitude ($\frac{1}{2}F/Oh\,k > 1$). The broken lines in figures 12(*a*) and 12(*b*) are two examples when this expression does not work; the initial disturbance amplitude is over predicted and the linear theory does not give the correct growth rate. Linear theory would not be expected to work well because the thin-filament equation predicts non-sinusoidal filament shapes at small times for large velocity modulation amplitudes.

An algebraic expression for the breakup time is possible using a modification of the above expression. The initial surface disturbance amplitude is always over predicted by the above expression for large values of velocity modulation amplitude. This over prediction can be corrected by multiplying (3*b*) by a single factor. This correction factor turns out to be 0.73.

The growth rate predicted by linear stability theory sometimes overestimates and sometimes underestimates the actual disturbance growth rate. Figures 12(*a*) and 12(*b*) are two examples of this behaviour. Linear stability theory would predict no disturbance growth at wavenumbers greater than one, which is contrary to the experimental results or the thin-filament equation results. The actual growth rate factor occurs at some wavenumber smaller than the current wavenumber. At large velocity modulation amplitudes, the growth factor goes to a limit. This limit is the value calculated at approximately a tenth of the initial wavenumber, which suggests a corrected wavenumber at which to calculate the disturbance growth factor. An empirical expression for this correct growth factor is

$$k_c = \tfrac{1}{10}k + (k - \tfrac{1}{10}k)(1 - \epsilon_0^n). \tag{7}$$

n is a parameter which controls the rate of change of the corrected wavenumber to the limiting values as the velocity modulation amplitude increases. A value of n that fits the data to the thin-filament equation is 0.33.

With the two above modifications, a new expression to predict breakup time is obtained:

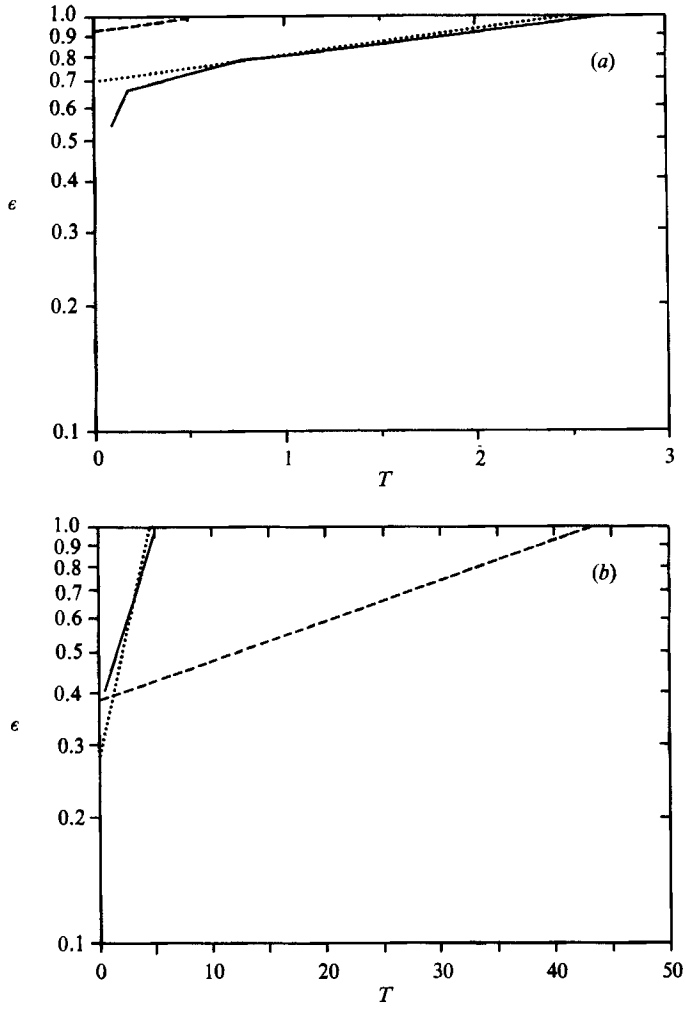

FIGURE 12. The growth of the surface disturbance amplitude with time. The solid line, broken line, and the dotted line are the results of the thin-filament equation, the expression by Bousfield & Denn, and (8), respectively, for (*a*) $k = 0.8$, $Oh = 0.89$, and $F = 23$; (*b*) $k = 0.89$, $Oh = 0.89$, and $F = 5$.

$$T_{\text{break}} = -\ln(\epsilon_{0c})/\gamma_c, \tag{8a}$$

$$\epsilon_{0c} = 0.73(1.0 - \exp(-F/12\,Oh\,k)), \tag{8b}$$

$$\gamma_c = [36k_c^4\,Oh^2 - 4k_c^2(1-k_c^2)]^{\frac{1}{2}} - 6k_c^2\,Oh, \tag{8c}$$

$$k_c = \tfrac{1}{10}k + (k - \tfrac{1}{10}k)(1 - \epsilon_0^{0.333}). \tag{8d}$$

The dotted lines in figures 8(*a–e*) and 12(*a*, *b*) illustrate the behaviour of this expression. The breakup time is predicted within 20 % of the thin-filament results for the entire range of Weber and Ohnesorge numbers studied. The disturbance growth rate factor does reduce to the linear stability result at low modulation amplitudes, but the initial surface disturbance amplitude does not reduce to the expression by Bousfield & Denn. The above expression is recommended when the group $F/12k\,Oh$ is greater than one.

7. Concluding remarks

At every value of the Ohnesorge number and the Weber number, there are regions of wavenumber and velocity modulation amplitude which produce uniform droplets. At low Ohnesorge numbers, uniform droplet production is limited mainly by satellite droplet formation. At high Ohnesorge numbers and high wavenumbers droplet production at a target size is constrained by droplet merging and unsteadiness: uniform droplets are produced but are twice as large as the modulation frequency would indicate. Satellite droplet volumes decrease with increasing Ohnesorge numbers. Satellite droplets are eliminated at Ohnesorge numbers greater than 1.6. Aerodynamic forces seem to be responsible for droplet merging and off-axis stray droplets.

The breakup length of viscous jets is predicted by the thin-filament equation within the scatter of the data. The maximum satellite volume size is predicted by the thin-filament equation. Satellite droplets merge under certain experimental conditions. The thin-filament equation predicts the elimination of satellite droplets at the correct Ohnesorge number.

An algebraic expression is presented to estimate the breakup times within 20% of the experimental data for viscous jets with a large initial modulation of the exit velocity. This expression works well for the entire range of collected data.

This research has been supported in part by the Department of Energy under contract No. AC02-83CE40626 and by a grant-in-aid from the American Paper Institute.

REFERENCES

Achenbach, E. 1974 Vortex shedding from spheres. *J. Fluid Mech.* **62**, 209.

Araki, N. & Kasuda, A. 1978 Production of droplets of uniform size by vibration. In *Proc. First Intl Conf. on Liquid Atomization and Spraying Systems*, vol. 8-1, p. 173.

Bogy, D. B. 1978 Use of one-dimensional Cosserat theory to study instability in a viscous liquid jet. *Phys. Fluids* **21**, 190.

Bogy, D. B. 1979*a* Breakup of a liquid jet: third perturbation Cosserat solution. *Phys. Fluids* **22**, 224.

Bogy, D. B. 1979*b* Drop formation in a circular liquid jet. *Ann. Rev. Fluid Mech.* **11**, 207.

Bogy, D. B., Shine, S. J. & Talke, F. E. 1980 Finite difference solution of the Cosserat fluid jet equations. *J. Comput. Phys.* **38**, 294.

Bousfield, D. W. 1988 Filament splitting between separating plates. *Chem. Engng Commun.* **73**, 19.

Bousfield, D. W. & Denn, M. M. 1987 Jet breakup enhanced by an initial pulse. *Chem. Engng Commun.* **53**, 219.

Bousfield, D. W., Keunings, R., Marrucci, G. & Denn, M. M. 1986 Nonlinear analysis of the surface tension driven breakup of viscoelastic filaments. *J. Non-Newtonian Fluid Mech.* **21**, 79.

Busker, D. P., Lamers, A. P. G. G. & Nieuwenhuizen, J. K. 1989 The non-linear break-up of an inviscid liquid jet using the spatial-instability method. *Chem. Engng Sci.* **44**, 377.

Chaudhary, K. C. & Maxworthy, T. 1980*a* The nonlinear capillary instability of a liquid jet. Part 2. Experiments on jet behaviour before droplet formation. *J. Fluid Mech.* **96**, 275.

Chaudhary, K. C. & Maxworthy, T. 1980*b* The nonlinear capillary instability of a liquid jet. Part 3. Experiments on satellite drop formation and control. *J. Fluid Mech.* **96**, 287.

Chaudhary, K. C. & Redekopp, L. G. 1980 The nonlinear capillary instability of a liquid jet. Part 1. Theory. *J. Fluid Mech.* **96**, 257.

Goedde, E. F. & Yuen, M. C. 1970 Experiments on liquid jet instability. *J. Fluid Mech.* **40**, 495.

GOLDIN, M., YERUSHALMI, J., PFEFFER, R. & SHINNAR, R. 1969 Breakup of a laminar capillary jet of viscoelastic fluid. *J. Fluid Mech.* **38**, 689.

GREEN, A. E. 1976 On the non-linear behavior of fluid jets. *Intl J. Engng Sci.* **14**, 49.

KEUNINGS, R. 1986 A transient finite element method for solving deformable surface flows. *J. Comput. Phys.* **62**, 199.

KURABAYASHI, T. & KARASAWA, T. 1982 Production of uniform droplets by non-circular nozzles. In *Proc. Second Intl Congr. on Liquid Atomisation and Spraying Systems*. Vol. 2–3, p. 55.

LAFRANCE, P. 1975 Nonlinear breakup of a laminar liquid jet. *Phys. Fluids* **18**, 428.

LEE, H. C. 1974 Drop formation in a liquid jet. *IBM J. Res. Dev.* **18**, 364.

LEIB, S. J. & GOLDSTEIN, M. E. 1986 The generation of capillary instabilities on a liquid jet. *J. Fluid Mech.* **168**, 479.

MCCARTHY, J. J. & MOLLOY, N. A. 1974 Review of stability of liquid jets and the influence of nozzle design. *Chem. Engng* **7**, 1.

NAYFEH, A. H. 1970 Nonlinear stability of a liquid jet. *Phys. Fluids* **13**, 841.

PAO, H. P. & KAO, T. W. 1977 Vortex structure in the wake of a sphere. *Phys. Fluids* **20**, 187.

PIMBLEY, W. T. & LEE, H. C. 1977 Satellite droplet formation in a liquid jet. *IBM J. Res. Dev.* **21**, 21.

PLATEAU, J. 1873 *Statique Experimentale et Theorique des Liquides Soumis aux Seules Forces Moleculaires*. Paris: Gauthier-Villars.

RAJAGOPALAN, R. & TIEN, C. 1973 Production of monodispersed drops by forced vibration of a liquid jet. *Can. J. Chem. Engng* **51**, 272.

RAYLEIGH, LORD 1879 On the instability of jets. *Proc. Lond. Math. Soc.* **10**, 4.

RUTLAND, D. F. & JAMESON, G. J. 1970 Theoretical prediction of the sizes of drops in the breakup of capillary jets. *Chem. Engng. Sci.* **25**, 1689.

RUTLAND, D. F. & JAMESON, G. J. 1971 A nonlinear effect in the capillary instability of liquid jets. *J. Fluid Mech.* **46**, 267.

SAKAI, T. , SADAKATA, M., SAITO, M., HOSHINO, N. & SENUMA, S. 1982 Uniform size droplets by longitudinal vibration of Newtonian and non-Newtonian fluids. In *Proc. Second Intl Conf. on Liquid Atomisation and Spraying Systems*, vol. 2, p. 37.

SCHNEIDER, J. M. & HENDRICKS, C. D. 1964 Source of uniform droplets. *Rev. Sci. Instrum.* **35**, 1349.

SCHUMMER, P. & TEBEL, K. H. 1982 *Germ. Chem. Engng* **5**, 209.

SHOKOOHI, F. 1976 Numerical investigation of the disintegration of liquid jets. Ph.D. thesis. Columbia University, New York. 132 pp.

STERLING, A. M. & SLEICHER, C. A. 1975 The instability of capillary jets. *J. Fluid Mech.* **68**, 477.

STOCKEL, I. H. 1988 Research on droplet formation for application to kraft black liquors. *Department of Energy Tech. Rep.* 4, DOE/CE/40626-T4.

TAUB, H. H. 1976 Investigation of nonlinear waves on liquid jets. *Phys. Fluids* **19**, 1124.

WANG, D. P. 1968 Finite amplitude effect on the stability of a jet of circular cross-section. *J. Fluid Mech.* **34**, 299.

WEAST, R. C. 1975 *Handbook of Chemistry and Physics*. Cleveland, Ohio: CRC Press.

WEBER, C. 1931 Zum Zerfall eines Flussigkeitsstrahles. *Z. Angew. Math. Mech.* **11**, 136.

YUEN, M. C. 1968 Non-linear capillary instability of a liquid jet. *J. Fluid Mech.* **33**, 151.